Probing Glycolytic and Membrane Potential Oscillations in *Saccharomyces cerevisiae*[†]

Allan K. Poulsen,*[,‡,§] Ann Zahle Andersen,[||] Jens Christian Brasen,[‡] Anne Marie Scharff-Poulsen,[§] and Lars Folke Olsen[‡]

CelCom, and Microbiology Group, Department of Biochemistry and Molecular Biology, University of Southern Denmark, Campusvej 55, DK-5230 Odense M, Denmark, and Risoe National Laboratory, Technical University of Denmark, Biosystems Department, Post Office Box 49, Frederiksborgvej 399, DK-4000 Roskilde, Denmark

Received March 7, 2008; Revised Manuscript Received May 13, 2008

ABSTRACT: We have investigated glycolytic oscillations under semi-anaerobic conditions in *Saccharomyces cerevisiae* by means of NADH fluorescence, measurements of intracellular glucose concentration, and mitochondrial membrane potential. The glucose concentration was measured using an optical nanosensor, while mitochondrial membrane potential was measured using the fluorescent dye $DiOC_2(3)$. The results show that, as opposed to NADH and other intermediates in glycolysis, intracellular glucose is not oscillating. Furthermore, oscillations in NADH and membrane potential are inhibited by the ATP/ADP antiporter inhibitor atractyloside and high concentrations of the ATPase inhibitor *N*,*N*′-dicyclohexylcarbodiimide, suggesting that there is a strong coupling between oscillations in mitochondrial membrane potential and oscillations in NADH mediated by the ATP/ADP antiporter and possibly also other respiratory components.

Yeast is one of the most well-studied organisms and is favored as a model system in many biochemical studies. It is easy to handle and displays many basic biochemical processes, which are mechanistically conserved in multicellular eukaryotes. Therefore, experimental results obtained by studies of yeast increase our understanding of complex metabolic networks in other eukaryotic cells, e.g., human cells.

In yeast cells, glycolysis is one of the most studied biochemical pathways. Nonetheless, while our understanding of the individual reaction steps in this pathway is significant, we have only limited knowledge about the overall behavior of the system, not only in yeast but also in a variety of different cell types. Glycolysis in yeast is known to oscillate under anaerobic (*1, 2*) or semi-anaerobic conditions (*3*). The latter implies that cyanide has been added to the cells to arrest respiration. Furthermore, it was recently shown that oscillations in glycolysis, as observed by oscillations in reduced nicotinamide adenine dinucleotide (NADH)[1] autofluorescence are accompanied by oscillations in mitochondrial membrane potential (*4*). The mechanism responsible for these membrane potential oscillations is not fully understood. This is mainly due to the fact that methods for real-time determination of metabolites in living cells are very scarce.

Methods for measurements of glucose in aqueous solution, for example, in blood plasma, are well-established. This is mainly due to the medical importance of such measurements, for example, in patients with diabetes mellitus. Such methods are often based on fluorescence (*5*), near-infrared (NIR) spectroscopy (*6, 7*), or enzymatic assays combined with electrochemical detection (*8–10*). However, none of these methods allows for real-time intracellular measurements of glucose in living cells. Information about intracellular metabolites is usually achieved by disruption of the cell, extraction of cell material, and subsequent analysis by the methods mentioned above. An alternative method to measure glucose is to use nanosensors (*11*). We have prepared nanosensors designed for real-time intracellular glucose measurements based on the design described by Xu et al. (*12*) and inserted them into yeast cells using electroporation. This allowed us to measure the time-resolved glucose concentration under conditions where glycolysis is oscillating (*13*). A somewhat unexpected result is that intracellular glucose appears not to oscillate but remains in a stationary state close to 0.5 mM. Furthermore, we have inserted the cyanine dye 3,3′-diethyloxacarbocyanine iodide [$DiOC_2(3)$] to measure oscillations in mitochondrial membrane potential, accompanying the oscillations in NADH. The oscillations in mitochondrial membrane potential are inhibited by the mitochondrial adenosine triphosphate (ATP)−adenosine diphosphate (ADP) antiport inhibitor atractyloside and high concentrations of dicyclohexylcarbodiimide (DCCD). The latter inhibits the proton translocating F_0F_1 ATPase at low concentrations but seems to have more unspecific effects on

[†] This research was supported by the Danish Natural Science Research Council (Grants 21-03-0132 and 272-05-0110), the Danish Medical Research Council (Grant 22-03-0336), the Lundbeck Foundation (Grant 102/05), and the Human Frontier Science Program (Grant RGP0041/2004C).

* To whom correspondence should be addressed. Telephone: +45-6550-2486. Fax: +45-6550-2467. E-mail: allanpoulsen@bmb.sdu.dk.

[‡] CelCom, University of Southern Denmark.

[§] Technical University of Denmark.

[||] Microbiology Group, Department of Biochemistry and Molecular Biology, University of Southern Denmark.

[1] Abbreviations: ADP, adenosine diphosphate; ATP, adenosine triphosphate; DCCD, dicyclohexylcarbodiimide; $DiOC_2(3)$, 3,3′-diethyloxacarbocyanine iodide; DLS, dynamic light scattering; FCCP, carbonyl cyanide *p*-trifluoromethoxyphenylhydrazone; NAD^+, nicotinamide adenine dinucleotide, oxidized form; NADH, nicotinamide adenine dinucleotide, reduced form; NIR, near-infrared.

10.1021/bi800396e CCC: $40.75
Published on Web 06/18/2008

respiration at higher concentrations (*14*) Our results suggest that the ATP−ADP antiport is involved in the coupling of oscillations of NADH to oscillations in mitochondrial membrane potential, but participation of other parts of the respiratory chain cannot be excluded.

MATERIALS AND METHODS

Chemicals and Reagents. All reagents were purchased from Sigma-Aldrich, Germany, unless otherwise noted. The reference dye Oregon Green dextran [molecular weight (MW) of 10 000 Da] and the fluorescent probe $DiOC_2(3)$ were purchased from Molecular Probes (Eugene, OR).

Synthesis of $Ru([dpp(SO_3Na)_2]_3)Cl_2 \cdot 6H_2O$. $RuCl_3$ (57 mg, 0.276 mmol) was reacted with 3.5 equiv of 4,7-diphenyl-1,10-phenanthroline disulfonic acid disodium salt (518 mg, 0.961 mmol) in 20 mL of distilled water and refluxed with stirring for 2 days. The solution color changed from dark green to red during this time. The solution was cooled and filtered. The solvent was removed by rotary evaporation, and the solid was redissolved in 5 mL of H_2O and loaded onto a Sephadex G25 size-exclusion column and eluted with H_2O. The first brown and purple fractions were discarded, and only the red band was collected. The red fraction was dried to give a red solid.

The product contains several isomers, with the $-SO_3Na$ substituents randomly positioned on the phenyl rings. However, previous reports indicate that the mixture of isomers gives no evidence of heterogeneous fluorescent lifetimes (*15*). Characterization of the compound by standard methods was performed as described in Castellano et al. (*16*).

Preparation of Glucose Nanosensors. The nanosensors were prepared by incorporation of the enzyme glucose oxidase, the oxygen-sensitive fluorescent dye $Ru([dpp(SO_3Na)_2]_3)Cl_2 \cdot 6H_2O$, and the oxygen-insensitive (*17*) fluorescent dye Oregon Green dextran into acrylamide polymerized in microemulsion as follows. A total of 2 mL of monomer solution was added dropwise into a solution of 43 mL of hexane, 3.08 g of AOT, and 1.59 g of Brij30 in a round-bottom flask. The monomer solution contained 2.7 g of acrylamide, 0.8 g of *N*,*N*′-methylenebis(acrylamide), and 9 mL of 10 mM sodium phosphate buffer at pH 7.2. A total of 12 μL of 10 mg/mL Oregon Green dextran, 20 μL of 60 mg/mL Ru complex, and 10 mg of glucose oxidase (∼200 units mg^{-1}) were added to the microemulsion (the compounds were dissolved in 10 mM sodium phosphate buffer at pH 7.2). The microemulsion was stirred under argon throughout the preparation and deoxygenated by three freeze−vacuum−thaw cycles using liquid nitrogen as the freezing medium. To initiate the polymerization, 50 μL of a 10% (w/w) sodium bisulfite solution was added. The solution was kept under argon and stirred at room temperature for 2 h to ensure complete polymerization. Hexane was removed by rotary evaporation, and the remaining solution was resuspended in 96% ethanol and transferred to an Amicon ultrafiltration cell model 8200 (Millipore Corp., Bedford, MA). The solution was washed with 600 mL of 96% ethanol to separate surfactants, unreacted monomers, excess proteins, and dyes from the sensors using a 100 kDa filter under 2 bar of pressure. The polymer particles containing Oregon Green dextran, glucose oxidase, and Ru complex were then resuspended in ethanol, passed through a suction filtration system (Millipore Corp., Bedford, MA), with a 0.025 μm nitrocellulose filter membrane, and rinsed with 100 mL of ethanol. The particles were collected when dry. The mean hydrodynamic particle diameter was 27 nm as determined by dynamic light scattering (DLS). The found particle size was similar to previous determinations obtained with DLS and atomic force microscopy (*18*). The diameter was determined by DLS at a fixed scattering angle of 90° using a BI-200SM goniometer from Brookhaven Instruments (New York), equipped with a 632.8 nm HeNe laser. The sample temperature was kept constant with a temperature-controlled water bath. Once the sensors were collected in the dried form, they could be stored for several months at −20 °C.

Insertion of Sensors. The glucose nanosensors were inserted into living yeast cells by electroporation using a gene pulser transfection apparatus equipped with a capacitor extender, both from Bio-Rad Laboratories, Hercules, CA. Nanosensors were prepared for insertion by dissolving them in 1 M sorbitol and sonicating for 30 min. Starved yeast cells were centrifuged for 3 min and suspended to 10% wet weight in the sorbitol solution containing sensors. A total of 400 μL of this solution was added to the electroporation cuvette with a gap of 0.2 cm. Electroporation was performed using a voltage of 450 V and a capacitance of 960 μF. After electroporation, the cells were centrifuged and washed 3 times in 10 mM sodium phosphate buffer at pH 7.2.

Mass Spectrometric Measurements of Oxygen Consumption and CO_2 *Production.* Measurements of oxygen consumption and CO_2 production were conducted using membrane inlet mass spectrometry as described in Poulsen et al. (*1*).

Fluorescence Measurements. Calibration of nanosensors and measurements of cells containing nanosensors were performed on an Edinburgh FS920 steady-state fluorometer (Edinburgh, Scotland). Oregon Green dextran and the Ru complex were both excited at 470 nm and emission was measured at 521 and 590 nm, respectively. The slits were set at 2.50 nm for both excitation and emission. The calibration was performed in a well-stirred (1250 rpm) 3 mL sample in contact with a gas headspace with a constant oxygen/nitrogen (21% oxygen) atmosphere. This ensured a homogeneous solution with an efficient supply of oxygen. Figure 1A shows the fluorescence spectra of the particles in the presence of different concentrations of glucose, while Figure 1B shows a plot of the ratio of the fluorescence peaks at 590 and 521 nm, respectively, against the concentration of glucose. The solid line represents a nonlinear fit of the data to a calibration curve defined by the equation

$$R = R_{\min} + \frac{R_{\max} - R_{\min}}{1 + 10^{(K_{\text{sensor}} - [\text{glucose}])}} \quad (1)$$

Here, R is the ratio of fluorescence peaks at 590 and 521 nm, respectively, R_{max} and R_{min} are constants, [glucose] is the glucose concentration, and K_{sensor} is a constant given by the sensor. It is worth noting that each new preparation of sensors showed a characteristic calibration curve that could be described by eq 1, but the constants R_{max}, R_{min}, and K_{sensor} may differ from one preparation to another. The response time of the sensor was estimated to about 40 s from measuring the time for the change from 10 to 100% of the response. This is a shorter response time than reported by

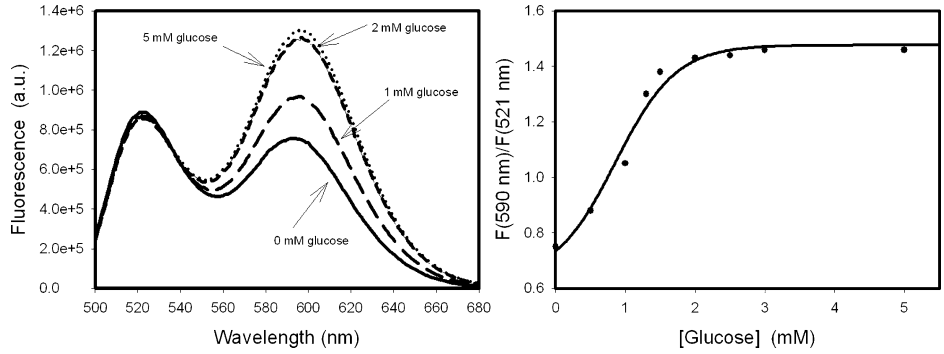

FIGURE 1: Calibration of glucose sensors in aqueous solutions containing various concentrations of glucose. (A) Spectra of sensors suspended in 10 mM potassium phosphate buffer at pH 7.2 containing different concentrations of glucose as indicated. The concentration of sensors was 2 mg/mL. Excitation wavelength = 470 nm. (B) Plot of the ratio of the fluorescence at 590 and 521 nm against the glucose concentration. The solid line represents a nonlinear fit to the data using eq 1. $R_{min} = 0.6312$, $R_{max} = 1.4777$, and $K_{sensor} = 0.8575$. Temperature = 25 °C.

Xu et al. (*12*), which could be explained by the smaller diameter of our nanosensors compared to those used by Xu et al. (*12*).

The principle of the sensors implies that glucose entering the sensor matrix is oxidized throught the reaction

$$\text{glucose} + O_2 \rightarrow \text{gluconic acid} + H_2O_2 \qquad (2)$$

catalyzed by glucose oxidase. The rate of depletion of oxygen is determined by the glucose concentration in the neighborhood of the sensor and is registered as an increase in the fluorescence by the oxygen-sensitive ruthenium dye in the matrix. Using membrane inlet mass spectrometry, we determined an overall oxygen consumption in a suspension of sensors supplied with glucose (data not shown) and, hence, the sensors can only be used to measure glucose in nonrespiring cells. Because oscillations in yeast cells are evoked here by the addition of cyanide to the yeast cell suspensions, no intracellular oxygen consumption because of oxidative phosphorylation will influence the measurements. Using membrane inlet mass spectrometry, we tested that respiration was inhibited 100%, in cells supplied with 5 mM potassium cyanide. Measurements of intracellular glucose in yeast were made under the same experimental conditions (volume, stirring rate, and temperature) as the in vitro calibrations of the sensors. Also, the concentrations of fluorophores in the yeast experiments were in the same concentration range as in the in vitro calibrations.

NADH autofluorescence (excitation at 366/3 nm and emission at 450/3 nm) and membrane potential-dependent $DiOC_2(3)$ fluorescence (excitation at 488/3 nm and emission at 600/3 nm) in yeast cells were also measured by the Edinburgh spectrofluorometer. The cells were suspended in a stirred 3 mL sample in a 1 × 1 × 4.5 cm quartz cuvette. When measuring mitochondrial membrane potential, the cells were supplied with 6 μM $DiOC_2(3)$ at time zero as described in ref *4*.

Yeast Cells. Yeast cells, *Saccharomyces cerevisiae* diploid strain X2180, were grown and harvested as described in Poulsen et al. (*1*).

RESULTS

We have used nanosensors to gain insight into glucose uptake and consumption in suspensions of yeast cells displaying oscillating glycolysis. The cells are small, and critical perturbations or even damage to the cells is a problem when it comes to quantitative determination of glucose uptake and intracellular concentration. One challenge is the insertion of sensors into cells. Yeast cells possess a rigid cell wall that has to be penetrated or circumvented in order to deliver material into the cells. Electroporation has previously been used successfully for insertion of material into yeast cells (*19*). Here, we demonstrate for the first time that polyacrylamide nanoparticles can be inserted into yeast cells using electroporation. Figure 2 shows the fluorescence spectra of a suspension of starved yeast cells into which we have inserted the glucose nanosensors, and it demonstrates that the incorporated nanosensors do indeed measure the uptake of glucose. The amount of glucose taken up 5 min after the addition of glucose corresponds to an intracellular concentration of about 0.5 mM (calculated by eq 1). Except for very low concentrations of extracellular glucose (<2 mM), the steady-state concentration of intracellular glucose was estimated to be around 0.5 mM, irrespective of the amount of glucose present in the suspension. This steady-state concentration of glucose was also independent of the cell density and amount of inserted glucose sensors (as determined by the fluorescence count per milligram of cells). To test

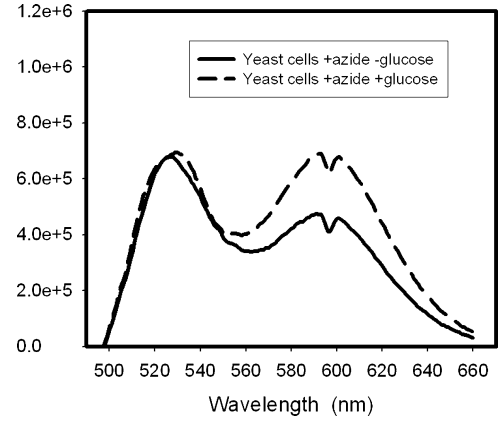

FIGURE 2: Fluorescence spectra of a suspension of starved yeast cells with incorporated glucose sensors before and after the addition of glucose to the external solution. Solid curve, spectrum of cells with incorporated glucose sensors in the presence of 5 mM sodium azide; dashed curve, spectrum of yeast cells with glucose sensors incorporated in the presence of 5 mM sodium azide and 5 min after addition of 10 mM glucose to the external medium. The curves emerge after subtraction of a background spectrum of yeast cells without sensors. Yeast cells corresponding to 5% wet weight were suspended in 10 mM phosphate buffer at pH 7.2 and 25 °C. Excitation wavelength = 470 nm.

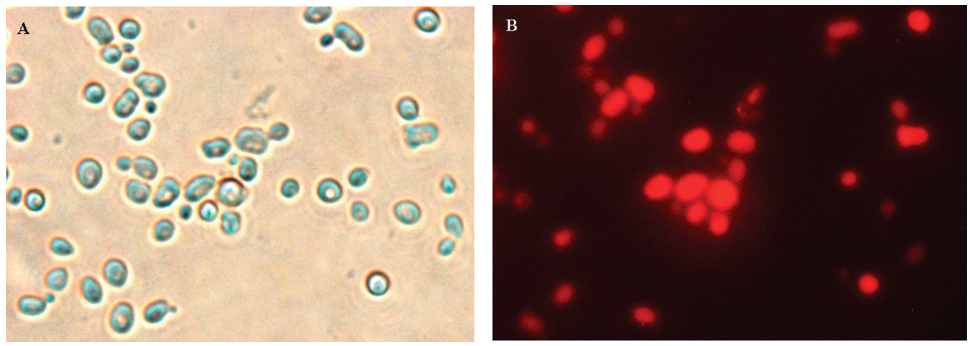

FIGURE 3: Yeast cells in which glucose sensors have been incorporated by electroporation. Yeast cells observed using (A) phase-contrast microscopy and (B) fluorescence microscopy. Approximately 50% of the cells show sensor fluorescence. Excitation at 450/50 nm and emission at 630/60 nm.

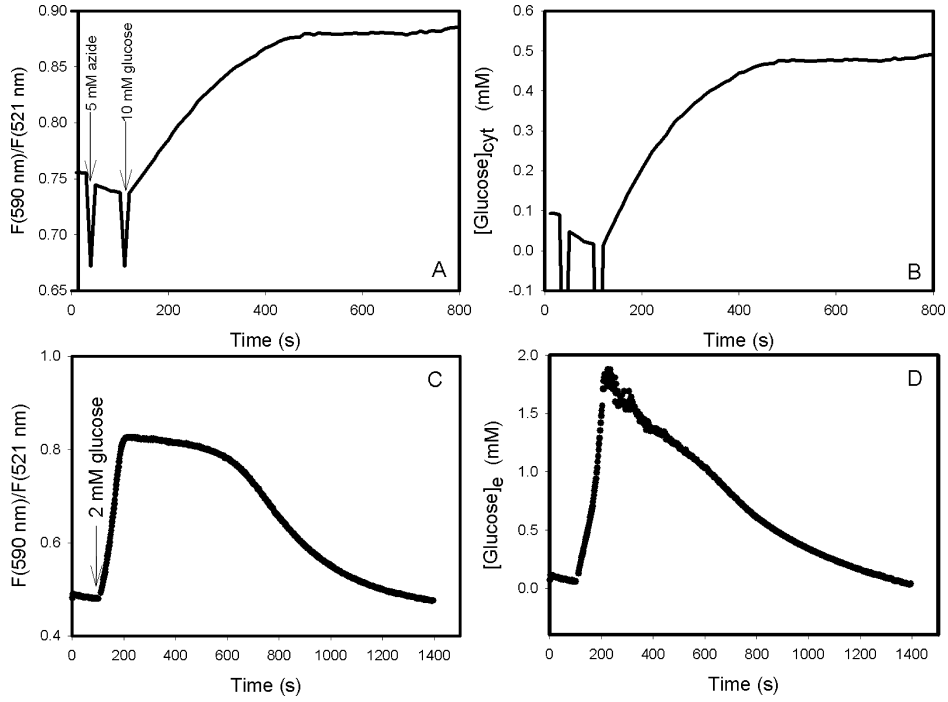

FIGURE 4: Kinetics of glucose uptake in starved yeast cells. (A) Ratio of emission wavelengths (excitation wavelength = 470 nm) because of incorporated glucose sensor in a suspension of starved yeast cells following the addition of first 5 mM sodium azide and then 10 mM glucose to the suspension. (B) Calculated intracellular glucose concentrations using the fluorescence data in A and the calibration function given by eq 1. (C) Glucose nanosensors are added to the extracellular medium and hence not inside the cells. The sensors react upon the addition of 2 mM glucose by an increase in the intensity ratio of the incorporated dyes. As the yeast cells use the glucose, the ratiometric signal returns to the baseline. (D) Calculated extracellular glucose concentration using fluorescence data in C. Starved yeast cells were suspended in 10 mM phosphate buffer at pH 7.2 to a density of 5% wet weight. Temperature = 25 °C.

whether the estimated steady-state concentration of around 0.5 mM represents a genuine intracellular concentration or it is a result of a change in the sensitivity of the sensors to glucose, we performed experiments where we added large amounts (~50 mM) of glucose to a suspension of cells where glucose consumption has been inhibited by either 20 mM of iodoacetate (*20*) or 5 mM of 2-deoxyglucose (*21*). We observed that the ratio of fluorescence at 590 nm over the 521 nm approached the saturation level of the sensor, meaning that the estimated glucose concentration, using a calibration curve as in Figure 5, increased to 5 mM or more (data not shown). Thus, we conclude that the estimated steady-state concentration in the absence of these inhibitors is a realistic value.

The yeast cells observed by phase contrast and fluorescence microscopy are shown in parts A and B of Figure 3, respectively. The fluorescence microscopy pictures reveal that the dye is evenly distributed in the cells. This uniform distribution of the glucose sensors can be seen for several hours after the insertion of the sensors. Figure 4 shows measurements of intracellular glucose concentration (Figure 4B) and glucose concentration in the external medium (Figure 4D) following a pulse of glucose; pulse sizes were 10 and 2 mM, respectively. The results demonstrate that the glucose sensors respond reversibly to changes in the glucose concentration.

The kinetics of glucose uptake in yeast cells was investigated by measuring the flux of glucose into the cells as a function of the concentration of glucose in the external medium. The respiration of the cells was inhibited by 5 mM sodium azide to avoid any interference of respiration and glucose consumption by the sensors. The data (not shown) obtained from these measurements could be fitted to a Michaelis−Menten type flux equation

$$J_0 = \frac{J_{max}[Glu]_e}{K + [Glu]_e} \quad (3)$$

where J_0 is the initial flux of glucose uptake, J_{max} is the maximum flux of glucose uptake (limited by the number of glucose transporter molecules in the plasma membrane), $[Glu]_e$ is the concentration of glucose in the extracellular medium, and K is the dissociation constant for the binding of glucose to the glucose transporter. We estimated values of $J_{max} = 2.2$ μM/s and $K = 15.7$ mM. The latter is within the previously reported range of 2−18 mM (*22–24*).

Thus, we were able to show that yeast cells with incorporated nanosensors take up glucose. However, it is obviously crucial to the results that the cells remain viable after electroporation. According to the literature, the viability of *S. cerevisiae* at the conditions used for insertion of nanosensors is approximately 95% (*19*) and sometimes up to 98% (*25*), subsequent to electroporation. We observed by microscopy that cells were able to divide after incorporation of nanosensors and the ability to form colonies when cultured on agar was unaltered (data not shown). It was also tested whether the cells with incorporated nanosensors were able to show oscillating glycolysis when pulsed with glucose and cyanide. In such a suspension, all cells oscillate in phase (*2, 26–28*).

Figure 5 shows temporal measurements of (A) the autofluorescence of NADH and (B) the intracellular concentration of glucose in a dense suspension of yeast cells with incorporated glucose sensors following the addition of first 30 mM glucose and then 5 mM cyanide to the suspension. We note that, while the concentration of NADH is oscillating in these cells, the concentration of glucose remains essentially constant around 0.4−0.5 mM.

We also investigated the coupling between the NADH oscillations and the oscillations in mitochondrial membrane potential discovered recently (*4*). Parts A and D of Figure 6 show plots of the NADH autofluorescence and the fluorescence as a result of $DiOC_2(3)$, which is an indicator of mitochondrial membrane potential. It was shown earlier that the addition of carbonyl cyanide *p*-trifluoromethoxyphenylhydrazone (FCCP), which uncouples the mitochondrial membrane proton gradient and hence uncouples oxidative phosphorylation, dissipates the mitochondrial membrane potential without affecting the oscillations in NADH (*4*). Furthermore, the addition of oligomycin, an inhibitor of F_0F_1 ATPase did not have an effect on neither the NADH oscillations nor the oscillations in membrane potential (data not shown). However, in some cases, yeast may carry resistance to oligomycin (*29*). Therefore, we first tested if oligomycin and other inhibitors were effective inhibitors of respiration of our yeast strain. This was performed in a membrane inlet mass spectrometer (*1*). We found that the addition of 50 μM oligomycin to a well-stirred suspension of yeast cells (10% wet weight) did not affect the respiration rate, whereas the addition of 300 μM atractyloside or 600 μM *N*,*N*′-dicyclohexylcarbodiimide (DCCD) both inhibited respiration by 20−50%, with atractyloside being the strongest inhibitor. At concentrations of DCCD around 5−10 μM, DCCD inhibits the F_0F_1 ATPase, but at higher concentrations (>20 μM), it inhibits mitochondrial respiration in a more unspecific manner (*14*). Atractyloside, on the other hand, is an inhibitor of the mitochondrial ADP/ATP antiporter.

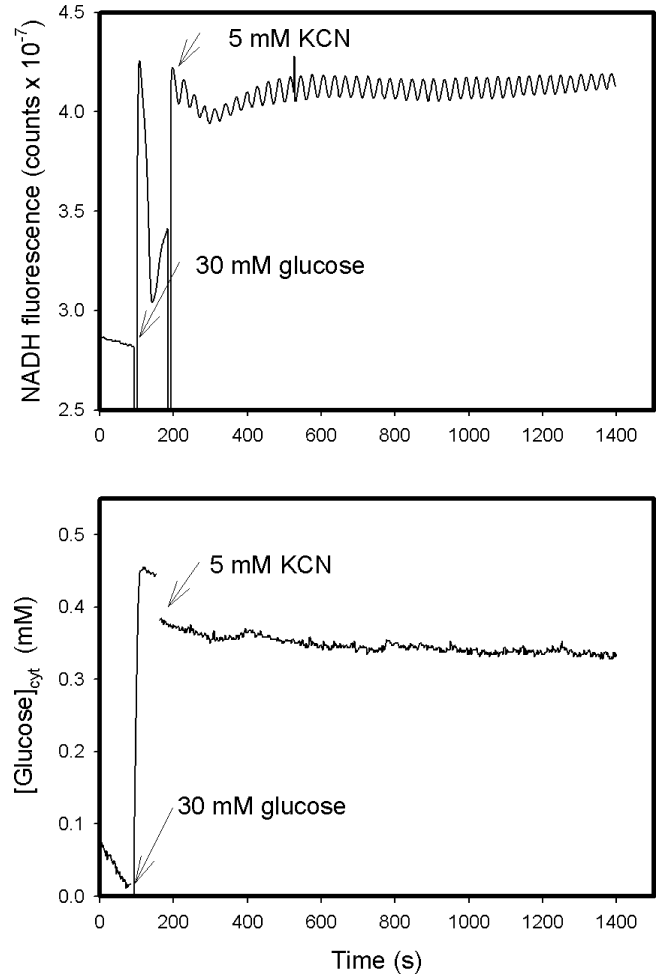

FIGURE 5: Real-time measurements of autofluorescence of NADH and intracellular concentration of glucose in a dense suspension of starved yeast cells following the addition of 30 mM glucose and subsequently 5 mM KCN. Yeast cells corresponding to a cell density of 10% wet weight and containing glucose nanosensors were suspended in 10 mM phosphate buffer at pH 7.2. Autofluorescence of NADH was measured at 450 nm (excitation wavelength = 366 nm). The intracellular glucose concentration was measured by the ratio of fluorescence at 590 and 521 nm (excitation wavelength = 470 nm) and converted to the glucose concentration using the calibration function given by eq 1. The temperature was 25 °C.

However, none of these inhibitors of respiration and oxidative phosphorylation were able to inhibit the respiration 100%. Parts B and E of Figure 6 show the effect of atractyloside on the oscillations of NADH and mitochondrial membrane potential, while parts C and F of Figure 6 show the effect of DCCD on these oscillations. Both inhibitors affect oscillations in NADH as well as oscillations in membrane potential. In the case of DCCD, the effect was only transient. The strongest effect seems to be that of atractyloside on mitochondrial membrane potential. It is interesting to note that the effect of these two inhibitors is the same on both NADH and membrane potential oscillations. In addition to inhibiting the oscillations in NADH and mitochondrial membrane potential, DCCD also seems to hyperpolarize the mitochondrial membrane potential. Finally, we tested the effect of amphotericin B on the oscillations in NADH and membrane potential. Amphotericin B forms channels in the plasma membrane and induces leakage of K^+. This outflux has been shown to induce a substantial decrease of some K^+-dependent glycolytic enzymes, such as aldolase, phosphofructokinase,

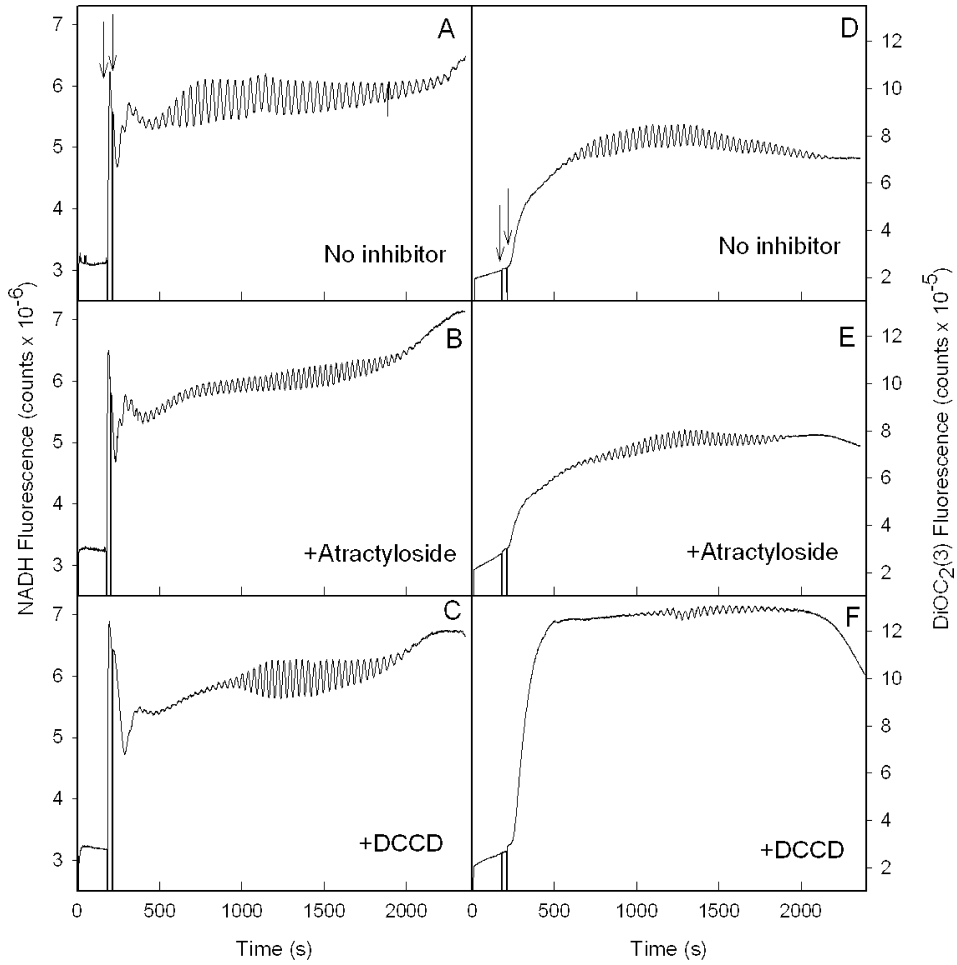

FIGURE 6: Oscillations in NADH (left panel) and mitochondrial membrane potential (right panel) in yeast cells supplemented with glucose and KCN and various inhibitors of oxidative phosphorylation. To a suspension of yeast cells (10% wet weight) were added 6 μM DiOC2(3) at time zero and 30 mM glucose at time 2.0 min followed by 5 mM KCN at time 2.5 min, indicated by arrows. In B and E, the cells were incubated with 300 μM atractyloside for 5 min before they were transferred to the cuvette in the spectrofluorometer, while in C and F, the cells were preincubated with 600 μM DCCD for 5 min. NADH is measured as fluorescence at 450 nm (excitation = 366 nm), and mitochondrial membrane potential is measured as fluorescence at 600 nm (excitation = 488 nm). The temperature was 25 °C.

and pyruvate kinase (*30*). The addition of 10 μM amphotericin B abolished oscillations of both NADH and membrane potential.

DISCUSSION

The use of different fluorescent probes allows us to get a deeper insight into the oscillations in NADH and mitochondrial membrane potential in yeast cells. The synthesis of nanosensors enables us to perform real-time measurements of intracellular concentrations of glucose in these cells. The fluorescence intensity of the Ru complex is affected by the partial pressure of oxygen in the environment of the nanoparticle. When glucose oxidase catalyzes the oxidation of glucose to gluconic acid, oxygen is consumed and the fluorescence of the Ru complex increases. As long as no fluorescent compound has been found, which is capable of selectively measuring the glucose concentration, the indirect method using the Ru complex offers a reliable method for glucose quantification in nonrespiring cells.

Insertion of two dyes into the polyacrylamide matrix allows for ratiometric measurements of glucose. The sensors can be calibrated *in vitro* and used directly *in vivo* by calculating the ratio of reporter peak intensity to the reference peak intensity. Furthermore, light scattering caused by the sample and fluctuations in excitation light intensity will not significantly affect the ratio of emitted light intensity [see for example Xu et al. (*12*)].

We have successfully inserted this sensor into yeast cells using electroporation and demonstrated that the cells are viable and fully functional after this treatment. Also, the sensors are fully functional after insertion. Viability of the electroporated yeast cells was confirmed by the ability of the cells to divide (observed by microscopy and colony formation on agar), to respond to glucose perturbation, and to perform glycolytic oscillations. The ability of the cells to perform glycolytic oscillations has been shown to be strongly dependent upon cell density (*31–33*). According to De Monte et al. (*33*) sustained oscillations vanishes at a cell density of $\approx 7 \times 10^8$ cells/mL. On the basis of the fact that cell density used in our experiments is approximately 1.2×10^9 cells/mL and that amplitude of the oscillations is almost unaffected by the presence of glucose sensors in the living cells, we conclude that cell viability following electroporation is high, which agrees with the findings of Weaver et al. (*19*) and Herman et al. (*25*).

Our measurements of the time-resolved glucose concentration in yeast cells with an oscillating glycolysis showed that, as opposed to the NADH concentration, the glucose con-

centration seems to be in a stationary state around 0.4−0.5 mM. It is concluded that the insertion of glucose nanosensors into the cells do not change the metabolism of the cells significantly, because the cells with incorporated glucose sensors show oscillations in NADH that are indistinguishable from oscillations in cells without glucose sensors. The oscillations in NADH and mitochondrial membrane potential are very sensitive to substances that affect the activity of glycolytic enzymes, such as amphotericin B (*30*). Thus, we conclude that the insertion of glucose sensors has no effect on the activity of glycolytic enzymes. Our measurements show that, following addition of more than 2 mM glucose to starved and nonrespiring yeast cells, the intracellular glucose concentration always approached a level of 0.4−0.5 mM, irrespective of the amount of added glucose. This estimate is independent of cell density. Furthermore, we determined the same steady-state concentration of glucose in cells with different amounts of sensors. Thus, any difference in the oxygen concentration between the extracellular phase and the cytoplasm must be negligible. Also, if the oxygen concentration in the cytoplasm were lower than in the extracellular space, our estimate of the intracellular glucose concentration would be an overestimate. The steady-state concentration of glucose of 0.5 mM must be limited by the glucose influx, because inhibiting glucose consumption by iodoacetate or 2-deoxyglucose results in an increase in the glucose concentration to 5 mM or higher. The sensors act reversibly and are able to respond to repeated increases and decreases of the glucose concentration (*12*). We found that the time for the sensors to respond to a change in the glucose concentration by a factor 10 is around 40 s. If intracellular glucose concentration does oscillate, it is expected that the amplitude must be very low. The periodicity of glycolytic oscillations is approximately 36 s (*34*) at 30 °C, and the sensor response time does not seem to be too high to detect small oscillations in intracellular glucose. The concentration of glucose determined in the present work agrees with the concentration predicted by models of glycolysis (*35, 36*) and with experimentally determined concentrations (*37–40*). It is important to emphasize that glucose concentrations determined in refs *37–40 are found in cell extracts, which do not allow for real-time quantification of intracellular glucose. Our work is thus the first report where nanosensors are inserted by use of electroporation and quantitative measurements of the kinetics and dynamics of glucose uptake in living yeast cells. However, the current sensor type has some drawbacks, such as acting irreversibly by consuming glucose and oxygen. The latter limits its use to nonrespiring cells. We are currently working on developing a new type of sensor that acts reversibly. Here, aptamers might show some use (41).*

The use of the membrane-potential-sensitive dye $DiOC_2(3)$ that specifically stains mitochondrial membranes shows that there is a coupling between the oscillations in the NADH concentration and oscillations in the mitochondrial membrane potential. We have shown previously that the addition of the uncoupler FCCP dissipates the membrane potential, while leaving the NADH oscillations unaffected (*4*). The addition of the inhibitors atractyloside and DCCD (instead of oligomycin) inhibits both the oscillations in NADH and mitochondrial membrane potential and essentially to the same extent. The effect of atractyloside suggests that the ADP/ATP antiporter is involved in the coupling of NADH and membrane potential oscillations. On the other hand, the effect of DCCD may be due to both an effect on the F_0F_1 ATPase and other components of the respiratory chain, e.g., the cytochrome bc_1 complex (*42*) or the plasma membrane H^+-ATPase (*43*). However, an interesting observation is that, while the amplitudes of the oscillations decrease after addition of atractyloside and DCCD, the period of the oscillations remain unaffected. This observation and the fact that NADH oscillations are unaffected by the uncoupler FCCP indicate that the oscillations in mitochondrial membrane potential are driven by the glycolytic oscillations.

ACKNOWLEDGMENT

The authors thank Anita Lunding for skilled technical assistance and Professor Olaf-Georg Issinger for inspiration and help with the Gene Pulser system. A.K.P. thanks Drs. Hao Xu and Raoul Kopelman for stimulating and useful discussions and their help and hospitality during a stay in the laboratory of Raoul Kopelman.

REFERENCES

1. Poulsen, A. K., Lauritsen, F. R., and Olsen, L. F. (2004) Sustained glycolytic oscillations—No need for cyanide. *FEMS Microbiol. Lett. 236*, 261–266.
2. Chance, B., Ghosh, A., and Estabrook, R. W. (1964) Damped sinusoidal oscillations of cytoplasmic reduced pyridine nucleotide in yeast cells. *Proc. Natl. Acad. Sci. U.S.A. 51*, 1244–1251.
3. Betz, A., and Chance, B. (1965) Influence of inhibitors and temperature on oscillation of reduced pyridine nucleotides in yeast cells. *Arch. Biochem. Biophys. 109*, 579–584.
4. Andersen, A. Z., Poulsen, A. K., Brasen, J. C., and Olsen, L. F. (2007) On-line measurements of oscillating mitochondrial membrane potential in glucose-fermenting *Saccharomyces cerevisiae*. *Yeast 24*, 731–739.
5. Pickup, J. C., Hussain, F., Evans, N. D., Rolinski, O. J., and Birch, D. J. S. (2005) Fluorescence-based glucose sensors. *Biosens. Bioelectron. 20*, 2555–2565.
6. Cui, H. X., Xu, K. X., Chen, M. S., and An, L. (2006) Temperature effect on the noninvasive measurement of human blood glucose by NIR. *Spectrosc. Spectral Anal. 26*, 838–841.
7. Arimoto, H., Tarumi, M., and Yamada, Y. (2003) Instrumental requirements for non-invasive blood glucose measurement using NIR spectroscopy. *Opt. Rev. 10*, 161–165.
8. Wilson, G. S., and Gifford, R. (2005) Biosensors for real-time in vivo measurements. *Biosens. Bioelectron. 20*, 2388–2403.
9. Meyerhoff, C., Mennel, F. J., Sternberg, F., Hoss, U., and Pfeiffer, E. F. (1996) Current status of the glucose sensor. *Endocrinologist 6*, 332–339.
10. Jung, S. K., Trimarchi, J. R., Sanger, R. H., and Smith, P. J. S. (2001) Development and application of a self-referencing glucose microsensor for the measurement of glucose consumption by pancreatic β-cells. *Anal. Chem. 73*, 3759–3767.
11. Almdal, K., Sun, H., Poulsen, A. K., Arleth, L., Jakobsen, I., Gu, H., and Scharff-Poulsen, A. M. (2006) Fluorescent gel particles in the nanometer range for detection of metabolites in living cells. *Polym. Adv. Technol. 17*, 790–793.
12. Xu, H., Aylott, J. W., and Kopelman, R. (2002) Fluorescent nano-PEBBLE sensors designed for intracellular glucose imaging. *Analyst 127*, 1471–1477.
13. Richard, P., Teusink, B., Westerhoff, H. V., and Vandam, K. (1993) Around the growth-phase transition *S. cerevisiaes* make-up favors sustained oscillations of intracellular metabolites. *FEBS Lett. 318*, 80–82.
14. Kovac, L., Galeotti, T., and Hess, B. (1968) Oligomycin-like inhibition of yeast respiration by *N*,*N*′-dicyclohexylcarbodiimide and nature of energy coupling in intact yeast cells. *Biochim. Biophys. Acta 153*, 715–717.
15. Anderson, S., Constable, E. C., Seddon, K. R., Turp, J. E., Baggott, J. E., and Pilling, M. J. (1985) Preparation and characterization of 2,2′-bipyridine-4,4′-disulphonic and bipyridine-5-sulfonic acids and their ruthenium(II) complexes—Excited-state properties and excited-

state electron-transfer reactions of ruthenium(II) complexes containing 2,2′-bipyridine-4,4′-disulphonic acid or 2,2′-bipyridine-4,4′-dicarboxylic acid. *J. Chem. Soc., Dalton Trans.* 2247–2261.

16. Castellano, F. N., and Lakowicz, J. R. (1998) A water-soluble luminescence oxygen sensor. *Photochem. Photobiol. 67*, 179–183.
17. Xu, H., Aylott, J. W., Kopelman, R., Miller, T. J., and Philbert, M. A. (2001) A real-time ratiometric method for the determination of molecular oxygen inside living cells using sol−gel-based spherical optical nanosensors with applications to rat C6 glioma. *Anal. Chem. 73*, 4124–4133.
18. Poulsen, A. K., Scharff-Poulsen, A. M., and Olsen, L. F. (2007) Horseradish peroxidase embedded in polyacrylamide nanoparticles enables optical detection of reactive oxygen species. *Anal. Biochem. 366*, 29–36.
19. Weaver, J. C., Harrison, G. I., Bliss, J. G., Mourant, J. R., and Powell, K. T. (1988) Electroporation−High-frequency of occurrence of a transient high-permeability state in erythrocytes and intact yeast. *FEBS Lett. 229*, 30–34.
20. Webb, J. L. (1966) *Enzyme and Metabolic Inhibitors*, Vol. 3, Academic Press, New York.
21. Herve, M., Wietzerbin, J., and Trandinh, S. (1993) Noncooperative effects of glucose and 2-deoxyglucose on their metabolism in *Saccharomyces cerevisiae* studied by ^{1}H NMR and ^{13}C NMR spectroscopy. *Eur. J. Biochem. 218*, 221–228.
22. Maier, A., Volker, B., Boles, E., and Fuhrmann, G. F. (2002) Characterisation of glucose transport in *Saccharomyces cerevisiae* with plasma membrane vesicles (countertransport) and intact cells (initial uptake) with single Hxt1, Hxt2, Hxt3, Hxt4, Hxt6, Hxt7 or Gal2 transporters. *FEMS Yeast Res. 2*, 539–550.
23. Bisson, L. F., Coons, D. M., Kruckeberg, A. L., and Lewis, D. A. (1993) Yeast sugar transporters. *Crit. Rev. Biochem. Mol. Biol. 28*, 259–308.
24. Smits, H. P., Smits, G. J., Postma, P. W., Walsh, M. C., and VanDam, K. (1996) High-affinity glucose uptake in *Saccharomyces cerevisiae* is not dependent on the presence of glucose-phosphorylating enzymes. *Yeast 12*, 439–447.
25. Herman, P., Drapalova, H., Muzikova, R., and Vecer, J. (2005) Electroporative adjustment of pH in living yeast cells: Ratiometric fluorescence pH imaging. *J. Fluoresc. 15*, 763–768.
26. Hess, B., and Boiteux, A. (1968) Mechanism of glycolytic oscillation in yeast. I. Aerobic and anaerobic growth conditions for obtaining glycolytic oscillation. *Hoppe−Seyler's Z. Physiol. Chem. 349*, 1567–1574.
27. Pye, E. K. (1969) Biochemical mechanisms underlying metabolic oscillations in yeast. *Can. J. Bot. 47*, 271–285.
28. Dano, S., Sorensen, P. G., and Hynne, F. (1999) Sustained oscillations in living cells. *Nature 402*, 320–322.
29. Parker, J. H., Trimble, I. R., and Mattoon, J. R. (1968) Oligomycin resistance in normal and mutant yeast. *Biochem. Biophys. Res. Commun. 33*, 590–595.
30. Wietzerbin, J., Herve, M., Lebourguais, O., and Trandinh, S. (1992) Comparative study of the effects of amphotericin B on the glucose metabolism in *Saccharomyces cerevisiae* in K^+-rich and Na^+-rich media. *Biochim. Biophys. Acta 1136*, 105–112.
31. Aldridge, J., and Pye, E. K. (1976) Cell density dependence of oscillatory metabolism. *Nature 259*, 670–671.
32. Aon, M. A., Cortassa, S., Westerhoff, H. V., and Vandam, K. (1992) Synchrony and mutual stimulation of yeast cells during fast glycolytic oscillations. *J. Gen. Microbiol. 138*, 2219–2227.
33. De Monte, S., d'Ovidio, F., Dano, S., and Sorensen, P. G. (2007) Dynamical quorum sensing: Population density encoded in cellular dynamics. *Proc. Natl. Acad. Sci. U.S.A. 104*, 18377–18381.
34. Poulsen, A. K., Petersen, M. Ø., and Olsen, L. F. (2007) Single cell studies and simulation of cell−cell interactions using oscillating glycolysis in yeast cells. *Biophys. Chem. 125*, 275–280.
35. Hynne, R., Dano, S., and Sorensen, P. G. (2001) Full-scale model of glycolysis in *Saccharomyces cerevisiae*. *Biophys. Chem. 94*, 121–163.
36. Wolf, J., Passarge, J., Somsen, O. J. G., Snoep, J. L., Heinrich, R., and Westerhoff, H. V. (2000) Transduction of intracellular and intercellular dynamics in yeast glycolytic oscillations. *Biophys. J. 78*, 1145–1153.
37. Teusink, B., Diderich, J. A., Westerhoff, H. V., van Dam, K., and Walsh, M. C. (1998) Intracellular glucose concentration in derepressed yeast cells consuming glucose is high enough to reduce the glucose transport rate by 50%. *J. Bacteriol. 180*, 556–562.
38. Clifton, D., Walsh, R. B., and Fraenkel, D. G. (1993) Functional studies of yeast glucokinase. *J. Bacteriol. 175*, 3289–3294.
39. Walsh, M. C., Smits, H. P., Scholte, M., and Vandam, K. (1994) Affinity of glucose transport in *Saccharomyces cerevisiae* is modulated during growth on glucose. *J. Bacteriol. 176*, 953–958.
40. De Koning, W., and Van Dam, K. (1992) A method for the determination of changes of glycolytic metabolites in yeast on a subsecond time scale using extraction at neutral pH. *Anal. Biochem. 204*, 118–123.
41. Hamula, C. L. A., Guthrie, J. W., Zhang, H. Q., Li, X. F., and Le, X. C. (2006) Selection and analytical applications of aptamers. *Trends Anal. Chem. 25*, 681–691.
42. Beattie, D. S., and Villalobo, A. (1982) Energy transduction by the reconstituted B−C1 complex from yeast mitochondria. *J. Biol. Chem. 257*, 4745–4752.
43. Velazquez, I., Martinez, F., and Pardo, J. P. (1997) Inactivation of the *Kluyveromyces lactis* H^+-ATPase by dicyclohexylcarbodiimide: Binding stoichiometry and effect of nucleophiles. *Arch. Biochem. Biophys. 346*, 294–302.

BI800396E